INVESTIGATION

Tunable Transcriptional Interference at the Endogenous Alcohol Dehydrogenase Gene Locus in *Drosophila melanogaster*

Victoria Jorgensen,* Jingxun Chen,*,[1] Helen Vander Wende,*,[1] Devon E. Harris,* Alicia McCarthy,† Shane Breznak,† Siu Wah Wong-Deyrup,† Yuzhang Chen,* Prashanth Rangan,† Gloria Ann Brar,* Eric M. Sawyer,*,[2] Leon Y. Chan,*,[2] and Elçin Ünal*,[2]

*Department of Molecular and Cell Biology, Barker Hall, University of California, Berkeley, CA, 94720 and †Department of Biological Sciences/RNA Institute, University at Albany SUNY, NY 12222

ORCID IDs: 0000-0002-4205-6198 (V.J.); 0000-0001-7320-8652 (J.C.); 0000-0002-0292-4528 (H.V.W.); 0000-0001-6406-1054 (D.E.H.); 0000-0002-7377-861X (Y.C.); 0000-0002-1452-8119 (P.R.); 0000-0003-1160-3838 (E.M.S.); 0000-0002-0189-4689 (L.Y.C.); 0000-0002-6768-609X (E.Ü.)

ABSTRACT Neighboring sequences of a gene can influence its expression. In the phenomenon known as transcriptional interference, transcription at one region in the genome can repress transcription at a nearby region in *cis*. Transcriptional interference occurs at a number of eukaryotic loci, including the alcohol dehydrogenase (*Adh*) gene in *Drosophila melanogaster*. *Adh* is regulated by two promoters, which are distinct in their developmental timing of activation. It has been shown using transgene insertion that when the promoter distal from the *Adh* start codon is deleted, transcription from the proximal promoter becomes de-regulated. As a result, the *Adh* proximal promoter, which is normally active only during the early larval stages, becomes abnormally activated in adults. Whether this type of regulation occurs in the endogenous *Adh* context, however, remains unclear. Here, we employed the CRISPR/Cas9 system to edit the endogenous *Adh* locus and found that removal of the distal promoter also resulted in the untimely expression of the proximal promoter-driven mRNA isoform in adults, albeit at lower levels than previously reported. Importantly, transcription from the distal promoter was sufficient to repress proximal transcription in larvae, and the degree of this repression was dependent on the degree of distal promoter activity. Finally, upregulation of the distal *Adh* transcript led to the enrichment of histone 3 lysine 36 trimethylation over the *Adh* proximal promoter. We conclude that the endogenous *Adh* locus is developmentally regulated by transcriptional interference in a tunable manner.

KEYWORDS
transcription
interference
Drosophila
Adh
CRISPR
Cas9
translation
chromatin
H3K36me3

Transcriptional interference, or *cis*-mediated downregulation of transcription at a locus as a result of transcription from a nearby location (Shearwin *et al.* 2005), was initially recognized as a mechanism of gene regulation conferred by retroviral promoters (Cullen *et al.* 1984). Since then, transcriptional interference has been observed to endogenously regulate genes in a number of eukaryotic contexts (Martens *et al.* 2004; Shearwin *et al.* 2005; Hongay *et al.* 2006; Bird *et al.* 2006; Hainer *et al.* 2011; van Werven *et al.* 2012; Yu *et al.* 2016). In particular, transcription of non-coding RNAs is widely associated with interference of promoters or regulatory elements of local coding transcripts (Martens *et al.* 2004; Hongay *et al.* 2006; van Werven *et al.* 2012; Yu *et al.* 2016; Kaikkonen and Adelman 2018).

In addition to non-coding RNAs, mRNA isoforms have also been linked to transcriptional interference. For genes with more than one promoter, transcription from the distal promoter may not only produce a distinct mRNA isoform, but could also lead to the repression of an mRNA isoform transcribed from the open reading frame (ORF)-proximal gene promoter (Corbin and Maniatis 1989; Moseley *et al.* 2002; Sehgal *et al.* 2008; Liu *et al.* 2015; Chen *et al.* 2017). In addition, since distinct mRNA isoforms may differ in their

doi: https://doi.org/10.1534/g3.119.400937
Manuscript received November 21, 2019; accepted for publication March 1, 2020; published Early Online March 25, 2020.

Supplemental material available at figshare: https://doi.org/10.25387/g3.10565984.
[1]These authors contributed equally to this work
[2]Corresponding author: E-mail: elcin@berkeley.edu

translational efficiency, regulation of promoter choice may impact gene expression at the protein level. In some instances, this difference in translational efficiency is due to the presence of upstream ORFs (uORFs) in the 5′ leader of the distal promoter-derived mRNA isoform, which could inhibit translation of the protein-coding ORF (Moseley *et al.* 2002; Law *et al.* 2005; Sehgal *et al.* 2008; Ingolia *et al.* 2011; Brar *et al.* 2012; Rojas-Duran and Gilbert 2012; Chew *et al.* 2016; Chen *et al.* 2017; Bird and Labbé 2017; Cheng *et al.* 2018; Zhang *et al.* 2018). As a result, in these cases, transcription of a distal promoter-derived mRNA isoform causes downregulation of protein expression through the integration of two seemingly disparate mechanisms of transcriptional and translational repression (Chen *et al.* 2017; Cheng *et al.* 2018; Van Dalfsen *et al.* 2018; Hollerer *et al.* 2019).

Transcription can antagonize downstream promoter activity by at least two means: First, the movement of the transcription machinery through the downstream promoter could interfere with transcription factor binding (Shearwin *et al.* 2005; van Werven *et al.* 2012; Zafar *et al.* 2014; Chia *et al.* 2017). Second, transcription through the downstream promoter could establish a repressive chromatin state (Hainer *et al.* 2011; van Werven *et al.* 2012; Woo *et al.* 2017; Chia *et al.* 2017). These mechanisms are not mutually exclusive and in fact have been shown to act in concert (van Werven *et al.* 2012; Chia *et al.* 2017). In the case of chromatin state changes, co-transcriptional histone modifications such as histone 3 lysine 36 trimethylation (H3K36me3) have been associated with nucleosome stabilization and repression of the downstream promoter (Hampsey and Reinberg 2003; Carrozza *et al.* 2005; Keogh *et al.* 2005; Houseley *et al.* 2008; Govind *et al.* 2010; van Werven *et al.* 2012; Ard and Allshire 2016; Chia *et al.* 2017). In metazoans, the link between H3K36me3 and transcription-coupled repression has been less clear. In mammalian cells, H3K36me3 has been implicated in Dnmt3b-dependent intragenic DNA methylation and suppression of cryptic transcription (Carvalho *et al.* 2013; Baubec *et al.* 2015; Neri *et al.* 2017). Reduction of H3K36me3 is lethal in *Drosophila* larvae and leads to elevated levels of histone 4 lysine 16 acetylation, a mark associated with active transcription (Bell *et al.* 2007; Meers *et al.* 2017). However, replacement of lysine 36 with a non-modifiable arginine (H3K36R) does not increase cryptic transcription initiation in fruit flies (Meers *et al.* 2017).

An established example of transcriptional interference in *Drosophila* is the regulation of the alcohol dehydrogenase (*Adh*) gene (Corbin and Maniatis 1989). *Adh* is transcribed from two closely positioned promoters, resulting in the production of at least two distinct mRNA isoforms (Figure 1A). These transcript isoforms are expressed in a developmentally regulated and tissue-specific manner (Ursprung *et al.* 1970; Benyajati *et al.* 1983; Savakis *et al.* 1986; Sofer and Martin 1987; Anderson *et al.* 1991; Visa *et al.* 1992). Transcription occurs from the ORF-proximal promoter (hereon referred to as *Adh* proximal promoter) during the early larval stages and from the ORF-distal promoter (hereon referred to as *Adh* distal promoter) during late third instar larvae and in adults (Figure 1B, adapted from Corbin and Maniatis, 1989 as well as Sofer and Martin 1987). It has been shown that transcription from the *Adh* distal promoter is necessary to repress transcription from the *Adh* proximal promoter (Corbin and Maniatis 1989). However, this previous study employed transgene insertions, and the same allele displayed variable degrees of transcriptional interference, attributed to positional effects (Corbin and Maniatis 1989). Therefore, both the impact and the extent of transcriptional interference at the endogenous *Adh* locus are currently unknown. It also remains to be tested whether the premature expression of the *Adh* distal transcript in larvae is sufficient to down-regulate the *Adh* proximal promoter. Furthermore, whether transcription from the *Adh* distal promoter is accompanied by downstream changes in H3K36me3 is unknown. Finally, the translational capacity of the two *Adh* mRNA isoforms has not been investigated. Here, we examined these unexplored aspects of *Drosophila Adh* regulation. We report that the transcriptional interference at the endogenous *Adh* locus is tunable and distal promoter activation is associated with H3K36me3 enrichment at the *Adh* proximal promoter. We further show that the two *Adh* transcript isoforms are both associated with high polysome fractions, indicating efficient translation.

MATERIALS AND METHODS

Fruit fly stocks, husbandry and larval collection

Fruit flies were raised on standard molasses medium at 25°. Oregon-R was used as wild type (a generous gift from Don Rio). The *tubGAL4* line was obtained from the Bloomington *Drosophila* Stock Center (ID 5138). All fruit flies in the stock were heterozygous for *tubGAL4* and the balancer *TM3*, Sb^1 Ser^1, as the *tubGAL4* chromosome is homozygous-lethal. For experiments requiring adult fruit flies, a mixture of males and females was used. The $Adh^{DIST\Delta}$ line was homozygous for the deletion allele. In experiments requiring induction of Adh^{DIST*} in larvae, we crossed homozygous Adh^{UAS} males to virgin female *tubGAL4/TM3*, Sb^1 Ser^1 or Oregon-R control fruit flies in collection cages with molasses plates spread with live yeast. After 8 hr, plates were removed, and embryos were allowed to age for 72 hr at 25°. The population consisted of predominantly first and second instar larvae. To collect the samples, larvae were washed off the plates using PBS and then washed three times in PBS. In between washes, larvae were left undisturbed to allow settling by gravity. ~2 mL of larvae were aliquotted, flash-frozen in liquid nitrogen, and stored at -80° for later processing.

Generation of transgenic fruit flies

We cloned sgRNAs into pCFD4 (Port *et al.* 2014), which expresses two sgRNAs from U6 snRNA promoters. Two sgRNAs were used to ensure that at least one double-stranded break was formed. The sgRNA plasmid for generating $Adh^{DIST\Delta}$ (pUB1041) expressed sgRNAs 5′-AGTGGGCTTGGTCGCTGTTG-3′ and 5′-TAATATAGAAAAAGCTTTGC-3′. The sgRNA plasmid for generating Adh^{UAS} (pUB1038) expressed sgRNAs 5′- CATAACTCGTCCCTGTTAAT-3′ and 5′-ACACATTTGTTAAAAGCATA-3′. The repair templates were cloned into the pGEX-2TK cloning vector (GE Healthcare). To generate the repair template for the $Adh^{DIST\Delta}$ allele (pUB1094), two 1-kb homology arms were amplified from Oregon-R genomic DNA, with the *Adh* distal promoter region removed. When used as a repair template donor, this results in the removal of the region spanning -387 to -1376 bp upstream of the proximal isoform transcriptional start site. A similar allele was described previously (Corbin and Maniatis 1989). The repair template to generate Adh^{UAS} (pUB1091) contained two 1-kb homology arms amplified from Oregon-R genomic DNA, flanking a *10xUAS-hsp70(core promoter)* construct amplified from pVALIUM20 (Ni *et al.* 2011). When used as a repair template donor, this results in the insertion of the *10xUAS-hsp70(core promoter)* construct at the -1 position relative to the distal transcriptional start site.

sgRNA plasmids and their corresponding repair templates were injected into y^1 *w M{nos-Cas9.P}ZH-2A* embryos (Bloomington 54591), which express maternal Cas9, by BestGene Inc. (Chino Hills, CA). The resulting mosaic fruit flies were outcrossed to w^{1118}, and the F_1 progeny were individually crossed to *CyO* or *CyO*, *twi* > *GFP*

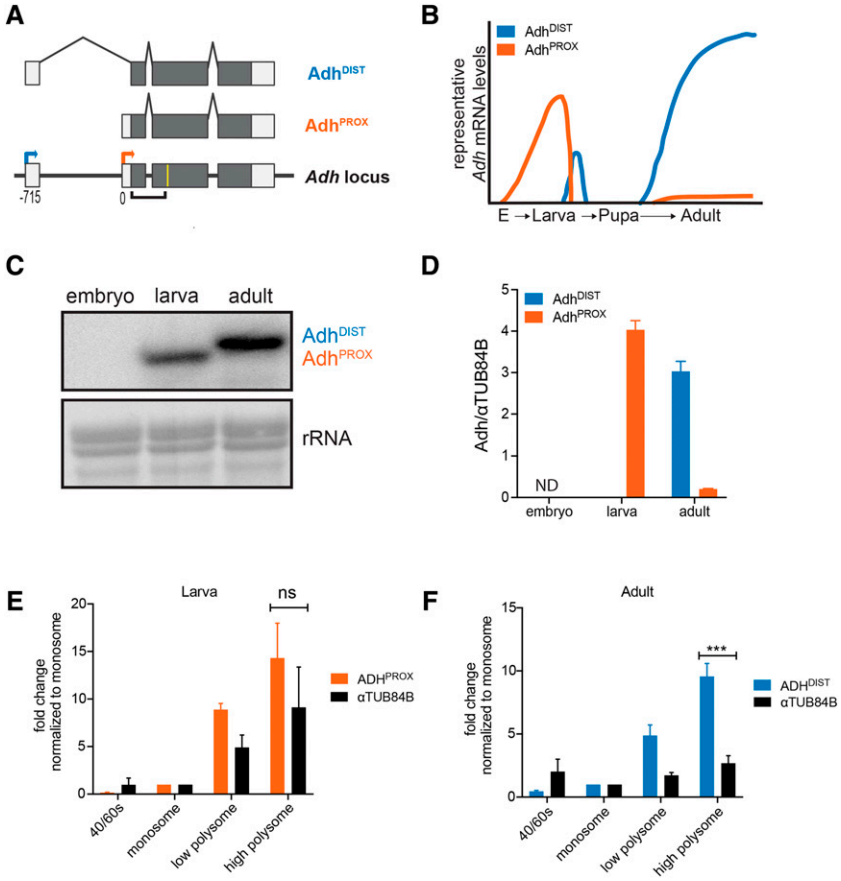

Figure 1 Transcription and translation of the two *Adh* isoforms during *Drosophila* development. (A) Illustration of coding (gray) and non-coding (white) exons of the *Adh* locus and the two *Adh* mRNA isoforms. Transcription of *Adh* can occur at either of two distinct transcription start sites (TSSs): the proximal TSS (orange arrow), nearest to the gene body, produces a short mRNA transcript (Adh^{PROX}), while the distal TSS (blue arrow), farthest from the gene body, produces a 5′ extended mRNA (Adh^{DIST}). Numbers below the *Adh* locus refer to distance in base pairs (bp) from the Adh^{PROX} TSS. The yellow line represents the relative location of the oligonucleotide probe used for RNaseH cleavage and the black-bracketed line represents the probe used in RNA blotting shown in (C). (B) Schematic adapted from Corbin and Maniatis 1989 and Sofer and Martin 1987 showing expression of *Adh* mRNA isoforms throughout development. (C) RNA blot of wild-type *Drosophila* RNA extracts throughout development confirms the stage-specific expression of both isoforms. Embryos were collected at 8 hr and L1/L2 larvae were collected at 72 hr. *Adh* transcripts were detected using a probe that hybridizes to a common region of all isoforms. Because the two isoforms vary by only ~50 bp, all samples were RNaseH cleaved in the second exon for better separation. Methylene blue staining of rRNA was used as a loading control. (D) Expression levels of Adh^{PROX} and Adh^{DIST} measured by RT-qPCR using isoform-specific primers. All data were normalized to a control αTUB84B transcript. The mean of two biological repeats from two separate collections is shown. Error bars represent the range. (E) and (F) RT-qPCR analysis of polysome profiles for Adh^{PROX} (orange), Adh^{DIST} (blue) and a control αTUB84B transcript (black) in wild-type L1/L2 larvae harvested at 80 hr (E) and wild-type adults (F). RNA was isolated individually from fractions and pooled into four categories: 40S/60S, monosome, low polysome (di- and trisome), high polysome (remaining fractions). Expression levels were obtained using isoform-specific primers and RT-qPCR. Data were first normalized to *in vitro* transcribed *RCC1*, which was spiked at equal amounts into each fraction prior to RNA extraction. Normalized data were then plotted relative to the amount present in the monosome fraction for each transcript. Data points represent the mean of 3 independent biological replicates. Error bars represent standard error of the mean (SEM). Two-tailed Student's *t*-test was used to calculate the p-values $^{***}P < 0.001$, n.s. not significant.

balancer lines prior to being genotyped. Introduction of the desired allele in the genotyped parent was tested by PCR and sequencing. F_2 progeny carrying the desired allele and balancer were then crossed *inter se* to generate homozygous animals.

RNA isolation, cDNA synthesis and quantitative PCR

Total RNA was isolated using TRIzol (Life Technologies) according to a previously described protocol (Bogart and Andrews 2006). 450 ng of isolated RNA was treated with DNase (TURBO DNA-free kit, Thermo Fisher) and reverse transcribed into cDNA (Superscript III Supermix, Thermo Fisher) according to the manufacturer's instructions. The RNA levels of specific *Adh* isoforms were quantified using primers specific to Adh^{DIST} and Adh^{PROX} (Table 1, supplemental file 1), SYBR Green/Rox (Thermo Fisher), and the StepOnePlus Real-time PCR system (Thermo Fisher). Adh^{DIST} and Adh^{PROX} signals were normalized to αTUB84B transcript levels. RT-qPCR for each sample was performed in technical triplicate and the mean Ct value was used for the normalizations. The efficiency value for each oligonucleotide pair was empirically determined and only those pairs that had greater than 90% efficiency were used for the RT-qPCR experiments. The oligonucleotide sequences used for the RT-qPCR experiments are displayed in Table 1, and primer efficiency calculations are shown in supplemental file 1. The raw Ct values and analyses for all the qPCR experiments are shown in supplemental files 2 through 6.

RNaseH digestion of total RNA

To distinguish the size difference between the two *Adh* isoforms, the total RNA of each sample was treated with RNaseH prior to RNA blot analysis. A total of 15 μg Trizol-extracted RNA was added to 1x RNaseH buffer (New England Biolabs, Ipswich, MA). Next, a site-specific DNA oligo (See Table 1 for sequence) was annealed to RNA by heating to 52° and slowly cooling to 25°. The RNA-DNA hybrid strands were incubated with 1 U RNaseH (New England Biolabs) for 1 hr at 37°. RNA was extracted in phenol:chloroform (1:1) and precipitated in isopropanol with 0.3 M sodium acetate overnight at -20°.

RNA blotting

RNA blot analysis protocol was performed as described previously (Koster *et al.* 2014) with minor modifications. 15 μg of total RNA was denatured in a glyoxal/DMSO mix (1 M deionized glyoxal, 50% v/v DMSO, 10 mM sodium phosphate (NaPi) buffer pH 6.5–6.8) at 70°

Table 1 Primers used in this study

Target gene	Primer	5′-3′ sequence
Adh (Northern Probe)	*Adh* probe F	ATCGAAAGAGCCTGCTAAAG
	Adh probe R	CCTTCAGCTCGGCAATGGCA
Adh (RNaseH)	*Adh* RNaseH oligo	GGTCACCTTTGGATTGATTG
Adh (RT-qPCR)	Adh^{PROX} forward	CCAACAACTAACGGAGCCCT
	Adh^{DIST} forward	GTTCAGCAGACGGGCTAACGAG
	Adh^{COMMON} reverse	GACCGGCAACGAAAATCACG
α*TUB84B* (RT-qPCR)	α*TUB84B* forward	GATCGTGTCCTCGATTACCGC
	α*TUB84B* reverse	GGGAAGTGAATACGTGGGTAGG
Adh (ChIP)	*Adh* A forward	GTGTGCCCTTTTGCTACTTAC
	Adh A reverse	GTTCAGCAGACGGGCTAACGAG
	Adh B forward	GAGGCCTGTTCCGCATATT
	Adh B reverse	GATAGCTAACGAAGGCACG
	Adh C forward	CTGAGCAGCCTGCGTACATA
	Adh C reverse	TGTCGGCCCCGTATTTATAG
	Adh D forward	CCAACAACTAACGGAGCCCT
	Adh D reverse	GACCGGCAACGAAAATCACG
	Adh E forward	TCCTGATCAACGGAGCTG
	Adh E reverse	GTCCCAGAAGTCCAGAATGG

for 10 min. Denatured samples were mixed with loading buffer (10% v/v glycerol, 2 mM NaPi buffer pH 6.5–6.8, 0.4% w/v bromophenol blue) and separated on an agarose gel (1.1–1.5% w/v agarose, 0.01 M NaPi buffer) for 3 hr at 116 V. The gels were then soaked for 25 min in denaturation buffer (0.05 N NaOH, 0.15 M NaCl), followed by 20 min in neutralization buffer (0.1 M Tris-HCl pH 7.5, 0.15 M NaCl). RNA was transferred to nitrocellulose membrane for 1 hr via vacuum transfer as described in Stratagene's Membranes Instruction Manual (Stratagene, La Jolla, CA). rRNA bands were visualized by methylene blue staining. The membranes were blocked in ULTRAhyb Ultrasensitive Hybridization Buffer (Thermo Fisher) for 3 hr before overnight hybridization. Membranes were washed twice in Low Stringency Buffer (2X SSC, 0.1% SDS) and three times in High Stringency Buffer (0.1X SSC, 0.1% SDS). All hybridization and wash steps were done at 42°. Radioactive probes were synthesized using a Prime-It II Random Primer Labeling Kit (Agilent, Santa Clara, CA). The oligonucleotide sequences of the primers used to generate the *Adh* DNA templates are listed in Table 1.

Rapid amplification of cDNA ends (5′ RACE) analysis

GeneRacer Kit Version L (Life Technologies) was used for full-length, RNA ligase-mediated rapid amplification of 5′ cDNA ends according to manufacturer's instructions. 2 μg of total RNA was isolated, as described above, from L1/L2 larvae and adults. The gene-specific primer used is listed in Table 1. A nested primer was not used. The resulting RACE products were analyzed and identified by DNA sequencing. Eight clones were analyzed and sequenced for each transcript isoform; failed sequencing reactions (no alignment) are not shown.

H3K36me3 and H3K4me3 chromatin immunoprecipitation (ChIP)

Chromatin immunoprecipitation in larval samples was performed as previously described (Alekseyenko *et al.* 2006) with the following modifications: Chromatin from approximately 2 mL of larval samples was isolated and fixed in 1.0% w/v of formaldehyde for 20 min at room temperature and quenched with 100 mM glycine. Crosslinked chromatin was sonicated 12 times with a 30 sec ON/30 sec OFF program using a Bioruptor Pico (Diagenode, Denville, NJ). A fragment size of ~200 bp was obtained. To preclear the lysate, the samples were incubated in pre-RIPA buffer (10 mM Tris-HCl pH 8.0, 1 mM EDTA, 0.1% SDS) containing cOmplete Protease Inhibitor Cocktail (Roche) and 1 mM PMSF with Protein A Dynabeads (Invitrogen) for 2 hr at 4° with rotation. After removal of Protein A Dynabeads, pre-cleared lysates were incubated overnight with 4 μg of anti-Histone H3K36me3 (Ab9050, Abcam), anti-Histone H3K4me3 (Ab8580, Abcam), or anti-Histone H3 (Ab1791, Abcam). Simultaneously, a new aliquot of Protein A Dynabeads were blocked in pre-RIPA buffer + 1 μg/μL bovine serum albumin overnight at 4°. The immunoprecipitates were then incubated with the pre-blocked Protein A Dynabeads for 4 hr at 4°. Reverse crosslinked immunoprecipitated DNA fragments were amplified with Absolute SYBR green (AB4163/A, Thermo Fisher, Waltham, MA) and quantified with a 7500 Fast Real-Time PCR machine (Thermo Fisher). The oligonucleotide sequences of the primers used for ChIP analysis are listed in Table 1. For quantification of enrichment, H3K4me3 and H3K36me3 signal was normalized to H3. Raw data for the qPCR analysis is shown in supplemental file 6.

Polysome fractionation and RNA extraction

Whole fruit flies or larvae harvested in 1X PBS were transferred to a microcentrifuge tube on liquid nitrogen. Samples were homogenized on ice in 200 μL cold lysis buffer in the presence of cycloheximide. The lysis buffer for cycloheximide samples is as follows: 500 mM KCl, 15 mM Tris-HCl pH 7.5, 15 mM $MgCl_2$, 0.5 mM Puromycin, 0.02 U SUPERaseIn, 1 cOmplete ULTRA EDTA-free protease inhibitor pill per 50 mL. Samples were centrifuged for 10 min at 15,000 g at 4°. The aqueous phase was transferred to a new pre-chilled microcentrifuge tube, avoiding the pellet and wax layer. 10% of the aqueous volume was transferred to a new microcentrifuge tube, with 100 μL TRIZol and stored at -80° for mRNA input sample. A 10% sucrose buffer (500 mM KCl, 15 mM Tris-HCl pH 7.5, 15 mM $MgCl_2$ and 7 μL SUPERaseIn) and 50% sucrose buffer (500 mM KCl, 15 mM Tris-HCl pH 7.5, 15 mM $MgCl_2$ and 7 μL SUPERaseIn) were used to generate a sucrose gradient of 10–40% in a Beckman Coulter 9/16x3.5 PA tube (Cat #331372) SW-41 ultracentrifugation tube. The gradient tube was stoppered and the setting "long sur 10-40%" was used to make the gradient. Gradients were centrifuged at 35,000 g using a SW-41 rotor for 3 hr at 4° and fractionated on a Brandel flow cell (Model #621140007) at 0.75 mL/min with the sensitivity setting at 0.5 Abs. A volume of 750 μL was collected for each fraction. The samples were then pooled as indicated

in Figure S1. 5 ng *rcc1*(xl)-polyA spike RNA was added to each pooled fraction prior to RNA extraction. RNA was extracted from the fractions using standard acid phenol:chloroform extraction as described in Chan *et al.* 2018. The RNA pellet was washed with 80% ethanol and then air-dried. After air-drying, the pellet was dissolved in 10 µl of nuclease-free water. The samples were then treated with Turbo DNase prior to cDNA synthesis.

Data availability

All the reagents generated in this study are available upon request. Supplemental material available at figshare: https://doi.org/10.25387/g3.10565984.

RESULTS

The *Adh* proximal promoter produces a transcript of 1001 nucleotides in length (hereon referred to as Adh^{PROX}), whereas the *Adh* distal promoter activates a transcription start site (TSS) located 715 base pairs (bp) upstream of the proximal TSS. The resulting transcript from the distal promoter, hereon referred to as Adh^{DIST}, has a unique 5′ leader located in exon 1 (Figure 1A, top). We first measured the relative abundance of the two *Adh* mRNA isoforms from wild-type embryos, larvae, and adult fruit flies using RNA blot hybridization. Because the two *Adh* isoforms differ by only 56 nucleotides, we employed an RNaseH digestion strategy to shorten the full-length transcripts so that a clear difference in isoform length could be detected (Figure 1A, yellow line marks the relative location of the oligonucleotide used for RNaseH digestion). Consistent with previous work (Savakis *et al.* 1986; Corbin and Maniatis 1989; diagrammed in Figure 1B), we observed that both *Adh* transcripts were undetectable in embryos (Figure 1C). Adh^{PROX} was expressed at high levels in early larval stages, and the Adh^{DIST} transcript was the predominant isoform in adults. To quantify the relative expression levels of each isoform, we used reverse transcription followed by quantitative polymerase chain reaction (RT-qPCR) using isoform-specific primers (supplemental file 1) and normalized Adh^{DIST} and Adh^{PROX} transcript measurements to αTUB84B, a ubiquitously expressed transcript. This analysis revealed that the Adh^{PROX} transcript level was ∼20 fold higher in larvae compared to in adults, whereas the Adh^{DIST} transcript had the reciprocal pattern with more than 8000-fold enrichment in adults compared to its expression level in larvae (Figure 1D, supplemental file 2). These data confirm that the *Adh* locus undergoes developmentally induced transcript isoform toggling, as evidenced by the mutually exclusive expression patterns of the two mRNA isoforms.

To determine the translational status of the two *Adh* isoforms, we enriched for ribosome-associated transcripts using sucrose gradient fractionation and measured the relative distribution of Adh^{PROX} or Adh^{DIST} across different fractions in larvae and whole adults. Adh^{PROX} was enriched in the high polysome fraction similar to αTUB84B (Figure 1E and Figure S1A, $P = 0.2$ two-tailed Student's *t*-test, supplemental file 3). Interestingly, in the adults, Adh^{DIST} enrichment in the high polysome fraction was more than fourfold higher relative to αTUB84B enrichment (Figure 1F and Figure S1B, $P = 0.0006$, two-tailed Student's *t*-test, supplemental file 3). We conclude that both Adh^{PROX} and Adh^{DIST} are well translated. Furthermore, Adh^{DIST} appears to be noticeably more enriched in the high polysome fractions than αTUB84B, indicating enhanced translational efficiency.

To assess the impact of transcriptional interference on Adh^{PROX} expression at the endogenous locus, we used CRISPR/Cas9-based editing (Jinek *et al.* 2012, 2013; Cong *et al.* 2013; Mali *et al.* 2013) to delete the *Adh* distal promoter (*Adh$^{DIST\Delta}$*) (Figure 2A and Figure S2A).

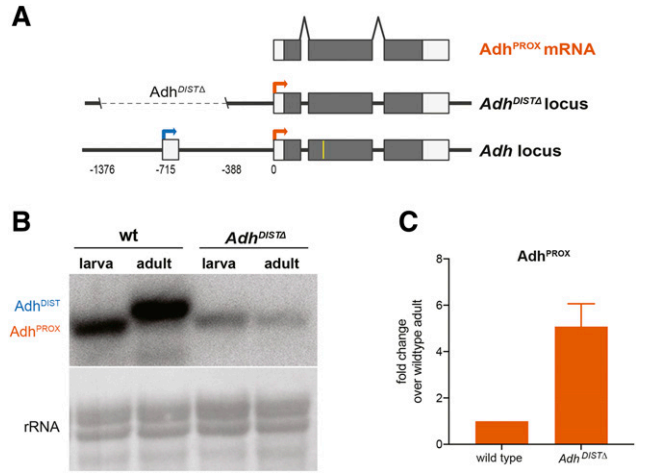

Figure 2 Deletion of the endogenous *Adh^{DIST}* promoter leads to Adh^{PROX} expression in adults. (A) Schematic of *Adh^{DIST}* promoter deletion, which will be referred to as *Adh$^{DIST\Delta}$*. Coding (gray) and noncoding (white) exons are shown. Arrows represent TSS of Adh^{PROX} (orange) and Adh^{DIST} (blue). Numbers below the *Adh* locus refer to distance in base pairs (bp) from the Adh^{PROX} TSS. The yellow line represents the relative location of the oligonucleotide probe used for RNaseH cleavage. (B) RNA blot in wild-type and *Adh$^{DIST\Delta}$* adult fruit flies and L1/L2 larvae. RNA isoforms were detected using a probe that hybridizes to a common region of all isoforms. Methylene blue staining of rRNA was used as a loading control. (C) Expression levels of Adh^{PROX} measured by RT-qPCR using isoform-specific primers. Data were first normalized to αTUB84B and then to wild-type adult levels. The mean of three independent biological replicates is shown. Error bars represent SEM.

Deletion of the *Adh* distal promoter resulted in a dramatic reduction of the Adh^{DIST} transcript and led to the expression of Adh^{PROX} in both larvae and adults, albeit at lower levels (Figure 2B and Figure S2B, supplemental file 4). RT-qPCR analysis showed a fivefold increase in Adh^{PROX} abundance in *Adh$^{DIST\Delta}$* mutants compared to wild-type adults (Figure 2C, supplemental file 4). We conclude that loss of transcription from the *Adh* distal promoter results in a modest de-repression of Adh^{PROX}, suggesting that, at least in adult fruit flies, transcription from the *Adh* distal promoter antagonizes the activity of the *Adh* proximal promoter.

Next, we tested if untimely overexpression of Adh^{DIST} during larval development was sufficient to repress Adh^{PROX} expression. Employing a similar CRISPR/Cas9-based editing strategy, we replaced the endogenous *Adh* distal promoter with an inducible *10xUAS-hsp70* promoter (*Adh^{UAS}*, transcript produced from this promoter is referred to as Adh^{DIST*}) (Figure 3A). The *Adh^{UAS}* line was crossed to a *tub-GAL4* line, which exhibits ubiquitous Gal4 expression driven from the *αTub84B* promoter. In the F_1 larvae, we observed ∼3000-fold increase of the Adh^{DIST*} isoform compared to wild type, accompanied by ∼10-fold decrease in the Adh^{PROX} isoform (Figure 3B and 3C, supplemental file 5). We noticed that, in F1 larvae from the *Adh^{UAS}* lines, Adh^{DIST*} expression was apparent even without the *GAL4* driver, likely due to leaky expression from the *hsp70* promoter, located immediately upstream of the Adh^{DIST*} TSS (Figure 3C and Figure S3). Comparison of lines with and without *GAL4* thus allowed us to achieve a range of Adh^{DIST*} expression levels, which provided insight into the dose-dependent relationship between production of Adh^{DIST*} and Adh^{PROX}. We found that the degree of Adh^{DIST*} overexpression scaled with the degree of Adh^{PROX} repression: the more the distal promoter activity, the less the proximal transcript abundance (Figure 3C, supplemental file 5).

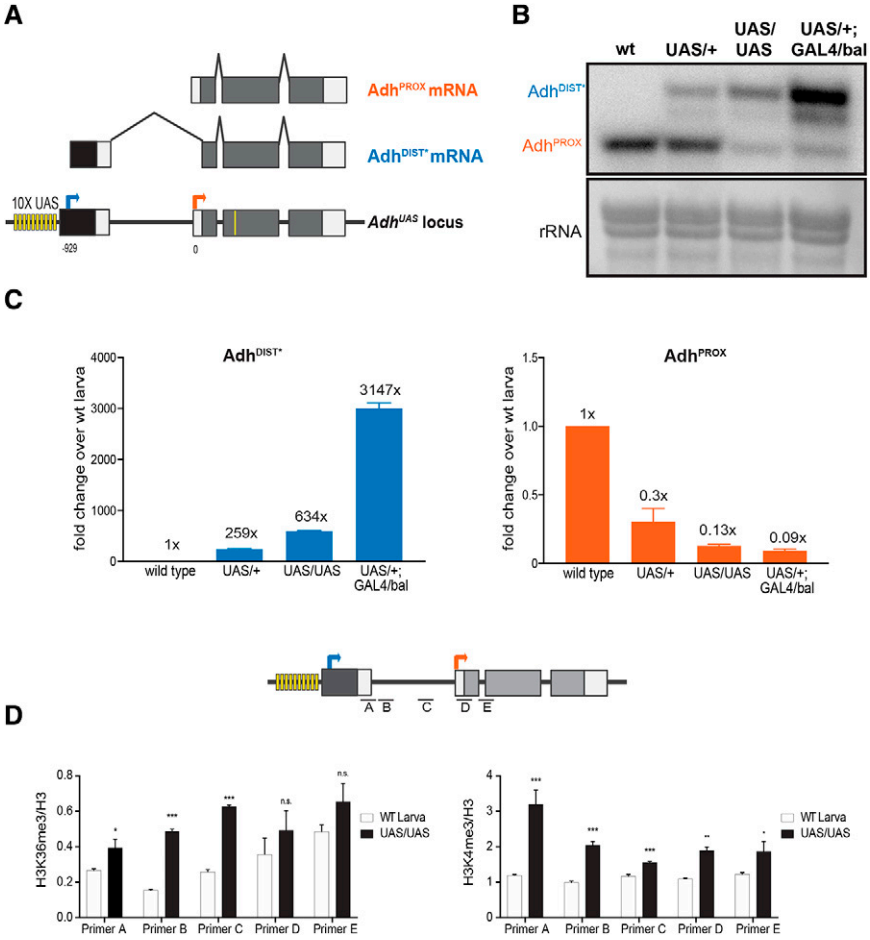

Figure 3 Ectopic expression of Adh^{DIST*} is sufficient for downregulation of Adh^{PROX} in larvae. (A) Diagram of GAL4/UAS induction system for *Adh*. Immediately upstream of the Adh^{DIST} TSS are 10 consecutive Gal4 bind sites (UAS) (shown as yellow bars) followed by the minimal *hsp70* promoter (shown in black). Coding (gray) and noncoding (white) exons are shown. Arrows represent TSSs of Adh^{PROX} (orange) and Adh^{DIST} (blue). The yellow line represents the relative location of the oligonucleotide probe used for RNaseH cleavage. Numbers below the *Adh* locus refer to distance in base pairs (bp) from the Adh^{PROX} TSS. The TSS for the GAL4-induced isoform (referred to as Adh^{DIST*}) was determined by 5′ RACE (Figure S3). (B) RNA blot analysis confirms that ectopic expression of Adh^{DIST*} in larvae is sufficient for Adh^{PROX} downregulation. RNA isoforms were detected using a probe that hybridizes to a common region of all isoforms. Methylene blue staining of rRNA was used as a loading control. (C) Expression levels of Adh^{DIST*} and Adh^{PROX} in larvae with varying degrees of Adh^{DIST} induction. Abundances of Adh^{DIST*} (left) and Adh^{PROX} (right) in larvae were measured for the following four lines: wild type, heterozygous UAS (UAS/+), homozygous UAS (UAS/UAS), heterozygous GAL4 and heterozygous UAS (UAS/+, GAL4/+). Expression levels were determined by RT-qPCR using isoform specific primers. All data were first normalized to αTUB84B and then to wild type (1x). The mean of three independent biological replicates is shown. Error bars represent SEM. (D) Induction of distal transcription promotes histone H3 lysine 36 trimethylation (H3K36me3) over the Adh^{PROX} promoter (left panel). Histone H3 lysine 4 trimethylation (H3K4me3) modifications, which are enriched at active promoters, are also shown (right panel). DNA recovered from chromatin IP were quantified using RT-qPCR and 5 primer pairs (A, B, C, D, and E) spanning the region between the *Adh* promoters as well as 5′ end of the gene body. All data were normalized to H3. Data points represent the mean of 3 independent biological replicates. Error bars represent SEM. Two-tailed Student's *t*-test was used to calculate the p-values $^{***}P < 0.001$, $^{**}P < 0.01$, $^{*}P < 0.05$, n.s. not significant.

This observation suggests that the antagonistic relationship between the levels of the two transcript isoforms is not binary, but tunable. RNA blotting confirmed that Adh^{DIST*} levels were highest in lines carrying the *GAL4* driver. Adh^{DIST*} was also expressed in *Adh^{UAS}* homozygous lines without the *GAL4* driver (Figure 3B). Even in the *Adh^{UAS}* heterozygous lines without the *GAL4* driver, Adh^{DIST*} expression in F_1 larvae was still higher than wild-type larvae, consistent with the RT-qPCR data (Figure 3B and 3C). We conclude that Adh^{DIST*} transcription is sufficient to downregulate Adh^{PROX} expression in a dose-dependent manner.

To test if transcription from the distal promoter led to changes in chromatin marks at the *Adh* locus, we performed chromatin immunoprecipitation (ChIP) against H3K36me3 and H3K4me3 in larvae collected from wild type and homozygous *Adh^{UAS}* lines, where both *Adh* alleles express Adh^{DIST*}. H3K36me3 is a co-transcriptionally established modification that occurs in regions downstream of active promoters (Xiao *et al.* 2003; Bannister *et al.* 2005; Mikkelsen *et al.* 2007) whereas H3K4me3 is highly enriched at active promoters near TSSs (Santos-Rosa *et al.* 2002). H3K4me3 enrichment was significantly increased near the Adh^{DIST*} transcription start site in the homozygous *Adh^{UAS}* line (Figure 3D, right panel, supplemental file 6), consistent with active transcription. Furthermore, a significant increase in H3K36me3 enrichment occurred over the *Adh* proximal promoter in these mutants (Figure 3D, left panel, supplemental file 6). We conclude that Adh^{DIST*} transcription is accompanied with increased H3K36me3 over the *Adh* proximal promoter, a chromatin mark that has been previously implicated in co-transcriptional repression in yeast and humans (Carrozza *et al.* 2005; Keogh *et al.* 2005; Carvalho *et al.* 2013).

DISCUSSION

The fruit fly *Adh* locus, which encodes alcohol dehydrogenase, is a well-established example of transcriptional interference. At the time that it was originally investigated, however, the locus was studied outside of its natural genomic context, using P element transgenes (Corbin and Maniatis 1989). Here, we revisit the regulation of this locus, leveraging CRISPR/Cas9-based editing, reverse transcription coupled with quantitative PCR, and chromatin immunoprecipitation to better define the regulation of this important gene. Although Adh^{PROX} is the predominant transcript isoform encoding the Adh enzyme during normal larval development, we demonstrate that the engineered induction of the Adh^{DIST} transcript is sufficient to repress Adh^{PROX} expression. Importantly, the degree of the distal promoter activity correlates well with the extent of transcriptional interference. Tunable transcriptional interference was first reported in bacteria

(Bordoy *et al.* 2016; Hao *et al.* 2016), more recently in yeast (Chia *et al.* 2017), and in human cells (Hollerer *et al.* 2019). All of these studies highlight the notion that gene regulation by transcriptional interference is not binary with an on/off state, but rather can be utilized to tune the expression of regulated mRNAs during developmental gene expression programs.

Even though the untimely expression of Adh^{DIST*} in larvae led to a significant decrease in Adh^{PROX} expression, the extent of repression (~10-fold) in the heterozygous *GAL4 Adh^{UAS}* line appears to be inconsistent with a *cis*-mediated transcriptional interference mechanism at a first glance. We attribute this unexpectedly high reduction of Adh^{PROX} level in the heterozygous lines to transvection, a common phenomenon in *Drosophila* in which interallelic promoters are co-regulated due to somatic pairing of homologous chromosomes. It has been shown that the GAL4-UAS system is subject to transvection (Mellert and Truman 2012; Noble *et al.* 2016). We consider that the transcription auxiliary factor(s) that activate the *UAS-hsp70* promoter also activate transcription from the wild-type *Adh* distal promoter on the homologous chromosome. As a result, the Adh^{PROX} expression can be downregulated by transcriptional interference even at the wild-type *Adh* locus in these heterozygous lines. Further tests are necessary to determine whether transvection plays a role in this context.

Although deletion of the *Adh* distal promoter at the endogenous locus de-repressed Adh^{PROX} expression in adult fruit flies, the severity of this phenotype was far less pronounced compared to a previous study (Corbin and Maniatis 1989). A possible explanation for this difference is that position effects arising from differences in P element transgene insertion sites might alter the levels of transcriptional interference that were observed. It is also possible that the transcriptional interference observed in transgene context might be elevated due to the sensitized system. Furthermore, the reduction of the Adh^{PROX} transcript in *Adh$^{DIST\Delta}$* larvae suggests that the deleted region carries sites for some as yet to be determined positive regulators for Adh^{PROX} expression. Alternatively, the deletion could change the nucleosome positioning in this region, which could impact Adh^{PROX} expression. Regardless of these points, our study demonstrates that at the endogenous *Adh* locus, distal promoter-driven transcriptional interference is necessary for Adh^{PROX} repression.

Our findings, in conjunction with the data reported in Corbin and Maniatis 1989, are consistent with a transcriptional interference-based mechanism operating at the *Adh* locus. However, alternative models could also explain why increased transcription from the distal *Adh* promoter in the UAS lines leads to a reduction in Adh^{PROX} expression. For instance, it is possible that a negative feedback mechanism could exist whereby increasing the expression of the Adh protein indirectly leads to a decrease in expression from the *Adh* proximal promoter. Overexpression of Adh protein from a transgene could help determine whether such a feedback mechanim indeed exists.

The regulation of the *Adh* gene described here has some similarities to that found for the *NDC80* gene in budding yeast (Chen *et al.* 2017; Chia *et al.* 2017). First, both genes have two promoters that are developmentally regulated, with the distal and proximal promoter encoding two distinct mRNA isoforms. Second, transcriptional interference is similar in both cases: transcription from the distal promoter is necessary and sufficient to repress the expression of the proximal promoter-derived isoform. Concomitant with this interference is the enrichment of H3K36me3 marks over the proximal promoter. While the H3K36me3 enrichment is similar between the cases of *Drosophila Adh* and yeast *NDC80*, we have been unable to assess causality in the current study. H3K36me3 is deposited by Set2, a highly conserved methyltransferase that physically associates with the elongating RNA polymerase II (Xiao *et al.* 2003). *Set2* is essential for the viability of the fruit fly (Bell *et al.* 2007). Our attempts to characterize Set2 involvement in *Adh* regulation using RNA interference were unsuccessful, since these lines did not survive to adulthood. This finding precluded us from determining the impact of H3K36me3 on Adh^{PROX} expression. Furthermore, the observation that replacement of H3 lysine 36 with arginine does not lead to increased cryptic transcription initiation (Meers *et al.* 2017) suggests that the co-transcriptional repression mechanism in *Drosophila* is more complex. Therefore, while the enrichment of H3K36me3 over the *Adh* proximal promoter correlates well with a decrease in Adh^{PROX} levels, this mark does not necessarily need to be involved in co-transcriptional repression in flies.

A key difference between examples of *Adh* and *NDC80* gene regulation is related to the translatability of the distal promoter-derived transcript isoforms. In the case of *NDC80*, the ORF within the distal promoter-derived mRNA is not translated, due to competing translation of multiple uORFs that are located in the 5′ leader of this transcript. The *NDC80* case thus shows an interesting link between transcriptional and translational regulation. In essence, production of the distal promoter-derived transcript results in both transcriptional and translational repression, ultimately resulting in decreased Ndc80 protein production. By contrast, the Adh^{DIST} transcript isoform is well translated, even better than the highly expressed αTUB84B transcript. The lack of translational repression in Adh^{DIST} is consistent with the absence of an AUG start codon within the 5′ leader of this transcript (Figure S3), thus excluding repressive uORF translation. The difference between the apparent regulation in these two cases is important: poor translation in the case of the 5′ extended *NDC80^{LUTI}* isoform and superior translation in the case of Adh^{DIST}. It is interesting to note that an earlier study, which examined the consequences of a natural transposon insertion at the *Adh* locus in the fruit fly (Dunn and Laurie 1995), along with a previous report (Laurie and Stam 1988), showed that the insertion of a *copia* retrotransposon between the *Adh* adult enhancer and the *Adh* distal promoter leads to an unusually low level of the Adh protein and enzyme activity. The reduction was found to occur as a result of a decrease in the level of the Adh^{DIST} transcript. Surprisingly though, in this case, the Adh^{PROX} transcript levels were proportionally increased in adults (Dunn and Laurie 1995). Given that the levels of the distal and proximal transcripts remain similar between the wild type and the lines carrying transposon insertion, these data suggest that in the adult fruit flies, Adh^{PROX} might not be as efficiently translated as Adh^{DIST}, which is consistent with our polysome analysis. One possibility is that tissue-specific, *trans*-acting factors could differentially modulate the translation of the two *Adh* mRNA isoforms. Such spatial effects are likely to be missed by the whole organism polysome fractionation approach that was used in this study.

More broadly, the switch from one mRNA isoform to another may alter not just the translational efficiency of the transcript, but also localization, stability, or alternative splicing as well. In this regard, transcript toggling driven by developmental switches in promoter usage and the subsequent transcriptional interference from distal gene promoters may serve to alter gene expression in respects other than gene silencing. We posit that the *Adh* example is likely to be one of many cases where developmentally controlled transcriptional interference from ORF-distal promoters can alter genome decoding and cellular function in a manner that has not been anticipated previously.

ACKNOWLEDGMENTS

V.J. performed the molecular biology experiments including RNA isolation, RNA blotting, cDNA synthesis, RT-qPCR, ChIP and 5′ RACE. J.C., H.V.W., D.E.H. and E.M.S. designed and generated the CRISPR/Cas9 transgenic lines, maintained the fruit fly stocks, and performed larval collection. Y.Z. assisted in the molecular biology experiments. L.Y.C. performed larval polysome fractionation. S.W.W., A.M., S.B. and P.R. performed the polysome fractionation experiments. E.Ü., L.Y.C. and E.M.S. supervised the project. V.J., J.C., H.V.W., E.M.S., L.Y.C., G.A.B. and E.Ü. wrote the manuscript. We would like to thank Qingqing Wang and Emily Brown for technical help and insight, Don Rio for comments on the manuscript, Jasper Rine for general advice and all members of the Brar and Ünal lab for comments and suggestions. The food for *Drosophila melanogaster* was prepared and provided by the UC Berkeley Biological Divisional Services Fly Food Facility. This work was supported by funds from the Pew Charitable Trusts (00027344), Damon Runyon Cancer Research Foundation (35-15), National Institutes of Health (DP2 AG055946-01) and Glenn Foundation for Medical Research to E.Ü.; funds from the Pew Charitable Trusts (00029624), the Alfred P. Sloan Foundation (FG-2016-6229), and the National Institutes of Health (DP2 GM-119138) to G.B.; funds from the Shurl and Kay Curci Foundation to L.Y.C.; an NSF Graduate Research Fellowship to J.C. (DGE-1106400) and an NSF Graduate Research Fellowship to E.M.S. (DGE 1752814 and DGE 1106400).

LITERATURE CITED

Alekseyenko, A. A., E. Larschan, W. R. Lai, P. J. Park, and M. I. Kuroda, 2006 High-resolution ChIP-chip analysis reveals that the Drosophila MSL complex selectively identifies active genes on the male X chromosome. Genes Dev. 20: 848–857. https://doi.org/10.1101/gad.1400206

Anderson, S. M., M. R. Brown, and J. F. McDonald, 1991 Tissue specific expression of the Drosophila Adh gene: a comparison of in situ hybridization and immunocytochemistry. Genetica 84: 95–100. https://doi.org/10.1007/BF00116548

Ard, R., and R. C. Allshire, 2016 Transcription-coupled changes to chromatin underpin gene silencing by transcriptional interference. Nucleic Acids Res. 44: 10619–10630. https://doi.org/10.1093/nar/gkw801

Bannister, A. J., R. Schneider, F. A. Myers, A. W. Thorne, C. Crane-Robinson *et al.*, 2005 Spatial Distribution of Di- and Tri-methyl Lysine 36 of Histone H3 at Active Genes. J. Biol. Chem. 280: 17732–17736. https://doi.org/10.1074/jbc.M500796200

Baubec, T., D. F. Colombo, C. Wirbelauer, J. Schmidt, L. Burger *et al.*, 2015 Genomic profiling of DNA methyltransferases reveals a role for DNMT3B in genic methylation. Nature 520: 243–247. https://doi.org/10.1038/nature14176

Bell, O., C. Wirbelauer, M. Hild, A. N. D. Scharf, M. Schwaiger *et al.*, 2007 Localized H3K36 methylation states define histone H4K16 acetylation during transcriptional elongation in Drosophila. EMBO J. 26: 4974–4984. https://doi.org/10.1038/sj.emboj.7601926

Benyajati, C., N. Spoerel, H. Haymerle, and M. Ashburner, 1983 The messenger RNA for alcohol dehydrogenase in Drosophila melanogaster differs in its 5′ end in different developmental stages. Cell 33: 125–133. https://doi.org/10.1016/0092-8674(83)90341-0

Bird, A. J., M. Gordon, D. J. Eide, and D. R. Winge, 2006 Repression of ADH1 and ADH3 during zinc deficiency by Zap1-induced intergenic RNA transcripts. EMBO J. 25: 5726–5734. https://doi.org/10.1038/sj.emboj.7601453

Bird, A. J., and S. Labbé, 2017 The Zap1 transcriptional activator negatively regulates translation of the RTC4 mRNA through the use of alternative 5′ transcript leaders. Mol. Microbiol. 106: 673–677. https://doi.org/10.1111/mmi.13856

Bogart, K., and J. Andrews, 2006 Extraction of Total RNA from Drosophila. CGB Technical Report 2006: 10. https://doi.org/10.2506/cgbtr-200610

Bordoy, A. E., U. S. Varanasi, C. M. Courtney, and A. Chatterjee, 2016 Transcriptional Interference in Convergent Promoters as a Means for Tunable Gene Expression. ACS Synth. Biol. 5: 1331–1341. https://doi.org/10.1021/acssynbio.5b00223

Brar, G. A., M. Yassour, N. Friedman, A. Regev, N. T. Ingolia *et al.*, 2012 High-resolution view of the yeast meiotic program revealed by ribosome profiling. Science 335: 552–557. https://doi.org/10.1126/science.1215110

Carrozza, M. J., B. Li, L. Florens, T. Suganuma, S. K. Swanson *et al.*, 2005 Histone H3 methylation by Set2 directs deacetylation of coding regions by Rpd3S to suppress spurious intragenic transcription. Cell 123: 581–592. https://doi.org/10.1016/j.cell.2005.10.023

Carvalho, S., A. C. Raposo, F. B. Martins, A. R. Grosso, S. C. Sridhara *et al.*, 2013 Histone methyltransferase SETD2 coordinates FACT recruitment with nucleosome dynamics during transcription. Nucleic Acids Res. 41: 2881–2893. https://doi.org/10.1093/nar/gks1472

Chan, L. Y., C. F. Mugler, S. Heinrich, P. Vallotton, and K. Weis, 2018 Non-invasive measurement of mRNA decay reveals translation initiation as the major determinant of mRNA stability. eLife 7. https://doi.org/10.7554/eLife.32536

Chen, J., A. Tresenrider, M. Chia, D. T. McSwiggen, G. Spedale *et al.*, 2017 Kinetochore inactivation by expression of a repressive mRNA. eLife 6. https://doi.org/10.7554/eLife.27417

Cheng, Z., G. M. Otto, E. N. Powers, A. Keskin, P. Mertins *et al.*, 2018 Pervasive, Coordinated Protein-Level Changes Driven by Transcript Isoform Switching during Meiosis. Cell 172: 910–923.e16. https://doi.org/10.1016/j.cell.2018.01.035

Chew, G.-L., A. Pauli, and A. F. Schier, 2016 Conservation of uORF repressiveness and sequence features in mouse, human and zebrafish. Nat. Commun. 7: 11663. https://doi.org/10.1038/ncomms11663

Chia, M., A. Tresenrider, J. Chen, G. Spedale, V. Jorgensen *et al.*, 2017 Transcription of a 5′ extended mRNA isoform directs dynamic chromatin changes and interference of a downstream promoter. eLife 6. https://doi.org/10.7554/eLife.27420

Cong, L., F. A. Ran, D. Cox, S. Lin, R. Barretto *et al.*, 2013 Multiplex Genome Engineering Using CRISPR/Cas Systems. Science 339: 819–823. https://doi.org/10.1126/science.1231143

Corbin, V., and T. Maniatis, 1989 Role of transcriptional interference in the Drosophila melanogaster Adh promoter switch. Nature 337: 279–282. https://doi.org/10.1038/337279a0

Cullen, B. R., P. T. Lomedico, and G. Ju, 1984 Transcriptional interference in avian retroviruses–implications for the promoter insertion model of leukaemogenesis. Nature 307: 241–245. https://doi.org/10.1038/307241a0

Dunn, R. C., and C. C. Laurie, 1995 Effects of a Transposable Element Insertion on Alcohol Dehydrogenase Expression in Drosophila Melanogaster. Genetics 140: 667–677.

Govind, C. K., H. Qiu, D. S. Ginsburg, C. Ruan, K. Hofmeyer *et al.*, 2010 Phosphorylated Pol II CTD recruits multiple HDACs, including Rpd3C(S), for methylation-dependent deacetylation of ORF nucleosomes. Mol. Cell 39: 234–246. https://doi.org/10.1016/j.molcel.2010.07.003

Hainer, S. J., J. A. Pruneski, R. D. Mitchell, R. M. Monteverde, and J. A. Martens, 2011 Intergenic transcription causes repression by directing nucleosome assembly. Genes Dev. 25: 29–40. https://doi.org/10.1101/gad.1975011

Hampsey, M., and D. Reinberg, 2003 Tails of intrigue: phosphorylation of RNA polymerase II mediates histone methylation. Cell 113: 429–432. https://doi.org/10.1016/S0092-8674(03)00360-X

Hao, N., A. C. Palmer, A. Ahlgren-Berg, K. E. Shearwin, and I. B. Dodd, 2016 The role of repressor kinetics in relief of transcriptional interference between convergent promoters. Nucleic Acids Res. 44: 6625–6638. https://doi.org/10.1093/nar/gkw600

Hollerer, I., J. C. Barker, V. Jorgensen, A. Tresenrider, C. Dugast-Darzacq *et al.*, 2019 Evidence for an Integrated Gene Repression Mechanism Based on mRNA Isoform Toggling in Human Cells. G3 (Bethesda) 9: 1045–1053. https://doi.org/10.1534/g3.118.200802

Hongay, C. F., P. L. Grisafi, T. Galitski, and G. R. Fink, 2006 Antisense transcription controls cell fate in Saccharomyces cerevisiae. Cell 127: 735–745. https://doi.org/10.1016/j.cell.2006.09.038

Houseley, J., L. Rubbi, M. Grunstein, D. Tollervey, and M. Vogelauer, 2008 A ncRNA Modulates Histone Modification and mRNA Induction in the Yeast GAL Gene Cluster. Mol. Cell 32: 685–695. https://doi.org/10.1016/j.molcel.2008.09.027

Ingolia, N. T., L. F. Lareau, and J. S. Weissman, 2011 Ribosome profiling of mouse embryonic stem cells reveals the complexity and dynamics of mammalian proteomes. Cell 147: 789–802. https://doi.org/10.1016/j.cell.2011.10.002

Jinek, M., K. Chylinski, I. Fonfara, M. Hauer, J. A. Doudna *et al.*, 2012 A programmable dual-RNA-guided DNA endonuclease in adaptive bacterial immunity. Science 337: 816–821. https://doi.org/10.1126/science.1225829

Jinek, M., A. East, A. Cheng, S. Lin, E. Ma *et al.*, 2013 RNA-programmed genome editing in human cells. eLife 2: e00471. https://doi.org/10.7554/eLife.00471

Kaikkonen, M. U., and K. Adelman, 2018 Emerging Roles of Non-Coding RNA Transcription. Trends Biochem. Sci. 43: 654–667. https://doi.org/10.1016/j.tibs.2018.06.002

Keogh, M.-C., S. K. Kurdistani, S. A. Morris, S. H. Ahn, V. Podolny *et al.*, 2005 Cotranscriptional set2 methylation of histone H3 lysine 36 recruits a repressive Rpd3 complex. Cell 123: 593–605. https://doi.org/10.1016/j.cell.2005.10.025

Koster, M. J. E., A. D. Yildirim, P. A. Weil, F. C. P. Holstege, and H. Th. M. Timmers, 2014 Suppression of intragenic transcription requires the MOT1 and NC2 regulators of TATA-binding protein. Nucleic Acids Res. 42: 4220–4229. https://doi.org/10.1093/nar/gkt1398

Laurie, C. C., and L. F. Stam, 1988 Quantitative analysis of RNA produced by slow and fast alleles of Adh in Drosophila melanogaster. Proc. Natl. Acad. Sci. USA 85: 5161–5165. https://doi.org/10.1073/pnas.85.14.5161

Law, G. L., K. S. Bickel, V. L. MacKay, and D. R. Morris, 2005 The undertranslated transcriptome reveals widespread translational silencing by alternative 5′ transcript leaders. Genome Biol. 6: R111. https://doi.org/10.1186/gb-2005-6-13-r111

Liu, Y., I. Stuparevic, B. Xie, E. Becker, M. J. Law *et al.*, 2015 The conserved histone deacetylase Rpd3 and the DNA binding regulator Ume6 repress BOI1's meiotic transcript isoform during vegetative growth in Saccharomyces cerevisiae. Mol. Microbiol. 96: 861–874. https://doi.org/10.1111/mmi.12976

Mali, P., L. Yang, K. M. Esvelt, J. Aach, M. Guell *et al.*, 2013 RNA-Guided Human Genome Engineering via Cas9. Science 339: 823–826. https://doi.org/10.1126/science.1232033

Martens, J. A., L. Laprade, and F. Winston, 2004 Intergenic transcription is required to repress the *Saccharomyces cerevisiae SER3* gene. Nature 429: 571–574. https://doi.org/10.1038/nature02538

Meers, M. P., T. Henriques, C. A. Lavender, D. J. McKay, B. D. Strahl *et al.*, 2017 Histone gene replacement reveals a post-transcriptional role for H3K36 in maintaining metazoan transcriptome fidelity. eLife 6. https://doi.org/10.7554/eLife.23249

Mellert, D. J., and J. W. Truman, 2012 Transvection Is Common Throughout the *Drosophila* Genome. Genetics 191: 1129–1141. https://doi.org/10.1534/genetics.112.140475

Mikkelsen, T. S., M. Ku, D. B. Jaffe, B. Issac, E. Lieberman *et al.*, 2007 Genome-wide maps of chromatin state in pluripotent and lineage-committed cells. Nature 448: 553–560. https://doi.org/10.1038/nature06008

Moseley, J. L., M. D. Page, N. P. Alder, M. Eriksson, J. Quinn *et al.*, 2002 Reciprocal Expression of Two Candidate Di-Iron Enzymes Affecting Photosystem I and Light-Harvesting Complex Accumulation. Plant Cell 14: 673–688. https://doi.org/10.1105/tpc.010420

Neri, F., S. Rapelli, A. Krepelova, D. Incarnato, C. Parlato *et al.*, 2017 Intragenic DNA methylation prevents spurious transcription initiation. Nature 543: 72–77. https://doi.org/10.1038/nature21373

Ni, J.-Q., R. Zhou, B. Czech, L.-P. Liu, L. Holderbaum *et al.*, 2011 A genome-scale shRNA resource for transgenic RNAi in Drosophila. Nat. Methods 8: 405–407. https://doi.org/10.1038/nmeth.1592

Noble, G. P., P. J. Dolph, and S. Supattapone, 2016 Interallelic Transcriptional Enhancement as an in Vivo Measure of Transvection in Drosophila melanogaster. G3 (Bethesda) 6: 3139–3148. https://doi.org/10.1534/g3.116.032300

Port, F., H.-M. Chen, T. Lee, and S. L. Bullock, 2014 Optimized CRISPR/Cas tools for efficient germline and somatic genome engineering in Drosophila. Proc. Natl. Acad. Sci. USA 111: E2967–E2976. https://doi.org/10.1073/pnas.1405500111

Rojas-Duran, M. F., and W. V. Gilbert, 2012 Alternative transcription start site selection leads to large differences in translation activity in yeast. RNA 18: 2299–2305. https://doi.org/10.1261/rna.035865.112

Santos-Rosa, H., R. Schneider, A. J. Bannister, J. Sherriff, B. E. Bernstein *et al.*, 2002 Active genes are tri-methylated at K4 of histone H3. Nature 419: 407–411. https://doi.org/10.1038/nature01080

Savakis, C., M. Ashburner, and J. H. Willis, 1986 The expression of the gene coding for alcohol dehydrogenase during the development of Drosophila melanogaster. Dev. Biol. 114: 194–207. https://doi.org/10.1016/0012-1606(86)90395-7

Sehgal, A., B. T. Hughes, and P. J. Espenshade, 2008 Oxygen-dependent, alternative promoter controls translation of tco1+ in fission yeast. Nucleic Acids Res. 36: 2024–2031. https://doi.org/10.1093/nar/gkn027

Shearwin, K. E., B. P. Callen, and J. B. Egan, 2005 Transcriptional interference – a crash course. Trends Genet. TIG 21: 339–345. https://doi.org/10.1016/j.tig.2005.04.009

Sofer, W., and P. F. Martin, 1987 Analysis of alcohol dehydrogenase gene expression in Drosophila. Annu. Rev. Genet. 21: 203–225. https://doi.org/10.1146/annurev.ge.21.120187.001223

Ursprung, H., W. Sofer, and N. Burroughs, 1970 Ontogeny and tissue distribution of alcohol dehyrogenase in Drosophila melanogaster. Dev. Genes Evol. 164: 201–208.

Van Dalfsen, K. M., S. Hodapp, A. Keskin, G. M. Otto, C. A. Berdan *et al.*, 2018 Global Proteome Remodeling during ER Stress Involves Hac1-Driven Expression of Long Undecoded Transcript Isoforms. Dev. Cell 46: 219–235.e8. https://doi.org/10.1016/j.devcel.2018.06.016

Visa, N., J. Fibla, M. C. Santa-Cruz, and R. Gonzàlez-Duarte, 1992 Developmental profile and tissue distribution of Drosophila alcohol dehydrogenase: an immunochemical analysis with monoclonal antibodies. J. Histochem. Cytochem. Off. J. Histochem. Soc. 40: 39–49. https://doi.org/10.1177/40.1.1729353

van Werven, F. J., G. Neuert, N. Hendrick, A. Lardenois, S. Buratowski *et al.*, 2012 Transcription of two long non-coding RNAs mediates mating type control of gametogenesis in budding yeast. Cell 150: 1170–1181. https://doi.org/10.1016/j.cell.2012.06.049

Woo, H., S. Dam Ha, S. B. Lee, S. Buratowski, and T. Kim, 2017 Modulation of gene expression dynamics by co-transcriptional histone methylations. Exp. Mol. Med. 49: e326. https://doi.org/10.1038/emm.2017.19

Xiao, T., H. Hall, K. O. Kizer, Y. Shibata, M. C. Hall *et al.*, 2003 Phosphorylation of RNA polymerase II CTD regulates H3 methylation in yeast. Genes Dev. 17: 654–663. https://doi.org/10.1101/gad.1055503

Yu, Y., R. M. Yarrington, E. B. Chuong, N. C. Elde, and D. J. Stillman, 2016 Disruption of promoter memory by synthesis of a long noncoding RNA. Proc. Natl. Acad. Sci. USA 113: 9575–9580. https://doi.org/10.1073/pnas.1601793113

Zafar, M. A., V. J. Carabetta, M. J. Mandel, and T. J. Silhavy, 2014 Transcriptional occlusion caused by overlapping promoters. Proc. Natl. Acad. Sci. USA 111: 1557–1561. https://doi.org/10.1073/pnas.1323413111

Zhang, H., S. Dou, F. He, J. Luo, L. Wei *et al.*, 2018 Genome-wide maps of ribosomal occupancy provide insights into adaptive evolution and regulatory roles of uORFs during Drosophila development. PLoS Biol. 16: e2003903. https://doi.org/10.1371/journal.pbio.2003903

Communicating editor: J. Ma